Performance analysis of the *Ormia ochracea's* coupled ears

Murat Akcakaya[a] and Arye Nehorai[b]
Department of Electrical and Systems Engineering, Washington University in St. Louis, St. Louis, Missouri 63130

(Received 14 January 2008; revised 30 June 2008; accepted 7 July 2008)

The *Ormia ochracea* is able to locate a cricket's mating call despite the small distance between its ears compared with the wavelength. This phenomenon has been explained by the mechanical coupling between the ears. In this paper, it is first shown that the coupling enhances the differences in times of arrival and frequency responses of the ears to the incoming source signals. Then, the accuracy of estimating directions of arrival (DOAs) by the *O. ochracea* is analyzed by computing the Cramér–Rao bound (CRB). The differential equations of the mechanical model are rewritten in state space and its frequency response is calculated. Using the spectral properties of the system, the CRB for multiple stochastic sources with unknown directions and spectra is asymptotically computed. Numerical examples compare the CRB for the coupled and the uncoupled cases, illustrating the effect of the coupling on reducing the errors in estimating the DOAs.
 [DOI: 10.1121/1.2967862]

PACS number(s): 43.60.Jn, 43.80.Lb [JAS] Pages: 2100–2105

I. INTRODUCTION

Most available array processing methods employ the time differences of arrival between the elements of a sensor array to estimate the directions of arrival (DOAs) of the incoming waves. Since the performance of such arrays is directly proportional to the size of the array's aperture, large aperture arrays are often required. However, this is costly and may be impractical in many tactical and mobile applications. This paper demonstrates a high-performance array with very small aperture, namely, of the parasitic fruit fly called the *Ormia ochracea*.

The *O. ochracea* is known to have a mechanical coupling between its ears to enhance its hearing. There are also other small animals having interactions between their ears for the same purpose,[1–5] but the mechanical coupling is unique for the *O. ochracea*. This coupling is necessary for the *O. ochracea's* perpetuation. The female *O. ochracea* must locate and deposit her parasitic maggots on or near a male field cricket, relying on the cricket's mating call, which is relatively pure in frequency (peak frequency 4.8 kHz). However, there is a tremendous incompatibility between the distance between the two ears ($\approx$1.2 mm) and the wavelength ($\approx$7 cm) of the cricket's mating call. This disaccord leads to extremely small interaural intensity and time of arrival differences between the ear closest to (ipsilateral) and the ear farthest from (contralateral) the sound source. It is believed that the coupling mechanism magnifies these binaural differences and subsequently improves the sound source localization accuracy.[3,6–10]

A mechanical system that models the mechanical coupling between the ears of the *O. ochracea* is introduced in Ref. 6. Miles *et al.*[6] showed experimentally that this model is well matched to the fly's ear in terms of frequency and transient responses.

In this paper, it is analytically shown that the mechanical coupling between the *O. ochracea's* ears is significant for localization accuracy. First, the system in Ref. 6 is represented in state space. Then the model is solved and its time and spectral properties are illustrated. The impulse response of the system is found, and after sampling it, by taking its discrete-time Fourier transform (DTFT), the frequency response is computed. The frequency and impulse responses for coupled and uncoupled versions of the system are compared to demonstrate the effect of coupling on the intensity and time differences between the two ears. A statistical model with multiple stochastic sources and measurement noise is then developed to analyze the effect of the coupling on localization performance. The asymptotic Cramér–Rao bound (CRB) on estimating the source DOA is computed in two-dimensional space, i.e., for simplicity the estimation of only the azimuth angle is considered. It is assumed that the DOA and the power spectra of the input signals are unknown. Finally, numerical examples that compare the CRB's of the coupled and the uncoupled systems are presented, showing the improvement in the localization accuracy due to coupling.

II. MODELING

In this section, a brief review of the anatomy of the female *O. ochracea's* ears is provided. The mechanical model used in Ref. 6 is described, associating its parameters with the parts of the ear. Then, to demonstrate the effect of the coupling, the impulse and frequency responses of the coupled and the uncoupled systems for a far-field source are computed and compared with each other.

Figure 1(a) shows the female *O. ochracea* and its ear structure. We observe the following.

[a]Electronic mail: makcak2@ese.wustl.edu
[b]Electronic mail: nehorai@ese.wust.edu

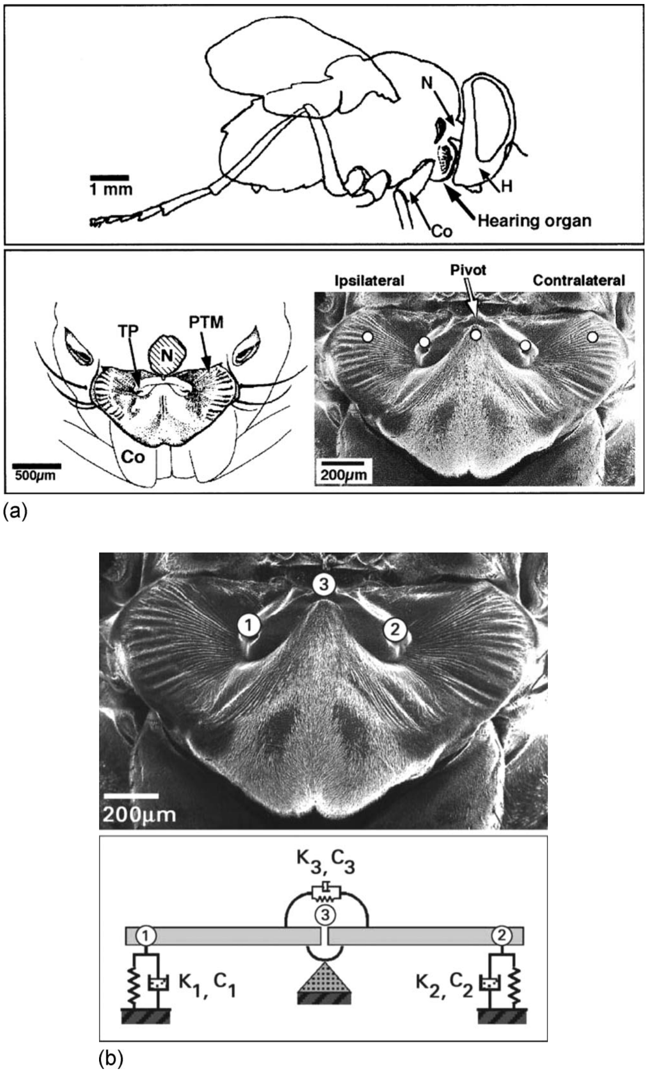

FIG. 1. (a) Anatomy of the female *Ormia ochracea's* ear. Top: side view of the *y*. Bottom: front view of the ear after the head was removed. (b) Top: front view of the ear after the head was removed. Bottom: mechanical model (Ref. 6).

- The ear is located on the front face of the thorax, which is behind the head.
- Prosternal tympanal membranes serve for hearing.
- Bulbae acustica (sensory organs) are connected to the tympanal pit.
- The tympanal pits and the pivot point are connected to each other by a cuticular structure referred as intertympanal bridge. This improves the usage of interaural differences.

A simple mechanical model, composed of springs and dash-pots, is proposed in Ref. 6 to explain the mechanical coupling between the ears [Fig. 1(b)] with k_i's and c_i's ($i=1,2,3$) as the spring and dash-pot constants, respectively. In this model, the intertympanal bridge is assumed to consist of two rigid bars connected at the pivot point through a coupling spring k_3 and dash-pot c_3. The springs and dash-pots at the extreme ends of the bridge approximately represent the dynamic properties of the tympanal membranes, bulbae acustica, and surrounding structures. The numerical values of the above model were empirically found for a 45° incident angle, but they were shown to hold also for a wide range of angles.[6]

The differential equations for the mechanical model in Fig. 1(b) can easily be written in matrix form following Ref. 6:

$$\begin{bmatrix} k_1+k_3 & k_3 \\ k_3 & k_2+k_3 \end{bmatrix}\begin{bmatrix} z_1(t) \\ z_2(t) \end{bmatrix} + \begin{bmatrix} c_1+c_3 & c_3 \\ c_3 & c_2+c_3 \end{bmatrix}\begin{bmatrix} \dot{z}_1(t) \\ \dot{z}_2(t) \end{bmatrix} + \begin{bmatrix} m & 0 \\ 0 & m \end{bmatrix}\begin{bmatrix} \ddot{z}_1(t) \\ \ddot{z}_2(t) \end{bmatrix} = \begin{bmatrix} f_1(t,\Delta) \\ f_2(t,\Delta) \end{bmatrix} = \boldsymbol{f}(t,\Delta), \tag{1}$$

where

- $f_i(t,\Delta)=p_i(t,\Delta)s$, $i=1,2$, where $p_1(t,\Delta)$ and $p_2(t,\Delta)$ both correspond to the same input sound source and are the pressure waves at the ipsilateral and the contralateral ears, respectively, and s is the surface area of each tympanal membrane (see Fig. 1);
- $z_1(t)$ and $z_2(t)$ are displacements at the first and second ends of the intertympanal bridge, respectively [see Fig. 1(b)];
- m is the effective mass of all moving elements and it is assumed to be concentrated at each end of the intertympanal bridge; and
- Δ corresponds to the time difference of arrival between the two ears: $\Delta=d\sin\phi/v$, where $\phi\in[-90°,90°]$ is the DOA, d is the distance between force locations, and v is the speed of sound, which is roughly 344 m/s.

In order to find the solutions for $z_1(t)$ and $z_2(t)$, Eq. (1) is rewritten as a state space model

$$\dot{\boldsymbol{x}}(t) = A\boldsymbol{x}(t) + B\boldsymbol{f}(t,\Delta),$$

$$\boldsymbol{y}(t) = C\boldsymbol{x}(t), \tag{2}$$

where $\boldsymbol{x}(t)=[x_1(t),x_2(t),x_3(t),x_4(t)]^T=[z_1(t),z_2(t),\dot{z}_1(t),\dot{z}_2(t)]^T$ is the state variable vector, A and B are constant matrices, which are functions of the model parameters in Eq. (1), and C is a constant matrix depending on the observations; see, for example, Ref. 11. C is chosen such that $\boldsymbol{y}(t)=[y_1(t),y_2(t)]^T=[z_1(t),z_2(t)]^T$. Using the variation of constants formula,[12] the solution for the state space model can be computed by

$$\boldsymbol{x}(t) = \Phi(t,t_0)\boldsymbol{x}(t_0) + \int_{t_0}^{t}\Phi(t,\tau)B\boldsymbol{f}(\tau,\Delta)d\tau,$$

$$\boldsymbol{y}(t) = C\boldsymbol{x}(t). \tag{3}$$

Here, t_0 is the initial time referencing the instant when the input signal first arrives at the ipsilateral ear and $\Phi(t,t_0)$ is the transition matrix depending on the matrix A.

Figures 2–4 show the impulse, amplitude, and phase responses, respectively, for both the coupled and uncoupled systems. Figure 2 illustrates the impulse responses, $\boldsymbol{h}(t,\Delta)=[h_1(t,\Delta),h_2(t,\Delta)]^T$, calculated for $\phi=45°$ using Dirac delta function in Eq. (3) as an input. The responses $h_1(t,\Delta)$ and $h_2(t,\Delta)$ correspond to the ipsilateral and contralateral ears, respectively. It is apparent that the interaural differences be-

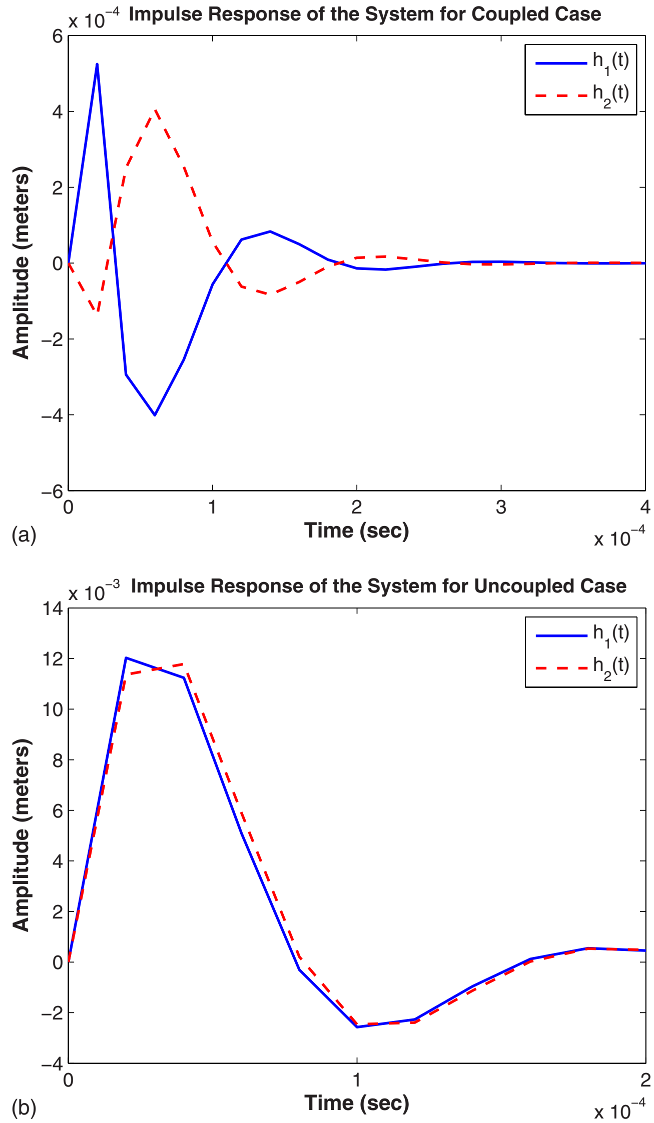

FIG. 2. (Color online) Impulse responses of the *Ormia ochracea's* two ears. (a) Coupled system. (b) Uncoupled system.

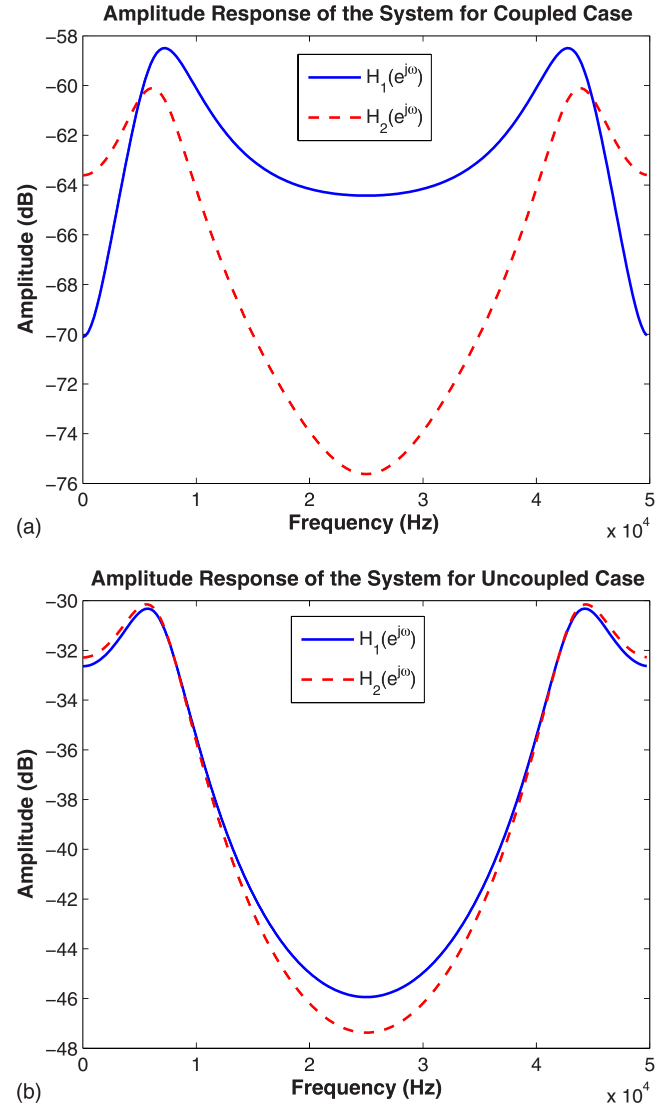

FIG. 3. (Color online) Amplitude responses of the *Ormia ochracea's* two ears. (a) Coupled system. (b) Uncoupled system.

tween the two ear outputs are enhanced for the coupled system [Figs. 2(a) and 2(b)]. These differences can be explained more clearly in the frequency domain. Therefore, the amplitude and phase responses are calculated by taking the DTFT (Ref. 13) of the sampled impulse responses. Figure 3 shows that the gap between the ipsilateral $(H_1(e^{j\omega},\Delta))$ and contralateral $(H_2(e^{j\omega},\Delta))$ amplitude responses is bigger for the coupled system [Figs. 3(a) and 3(b)]. This confirms the improvement of the intensity differences between the ear outputs. Similarly, Fig. 4 demonstrates how the phase difference between the responses of the two ears is amplified, so is the difference in the arrival time of the sound source to the two ears for coupled system [Figs. 4(a) and 4(b)]. This analysis may explain how the extremely small interaural differences in intensity and arrival time are increased by the coupling to a level that the *O. ochracea* could use the improved binaural cues to process the information more effectively.

III. PERFORMANCE ANALYSIS

In this section, a statistical model is presented and the CRB on DOA estimation of model (3) is computed.

A. Statistical model

The model consists of M multiple stochastic inputs $p_m(t)$ $(m=1,2,\ldots,M)$ and additive measurement noise $\boldsymbol{e}(t)=[e_1(t),e_2(t)]^T$ with $e_1(t)$ and $e_2(t)$ corresponding to the measurement noise at the ipsilateral and contralateral ears, respectively (Fig. 5). That is, M different angles for M different input signals are chosen to model the environment. This model gives rise to

$$\boldsymbol{y}(t,\boldsymbol{\Delta}) = \sum_{m=1}^{M} p_m(t) \times h(t,\Delta_m) + \boldsymbol{e}(t), \quad t=1,2,\ldots,N, \quad (4)$$

where $\boldsymbol{\Delta}=[\Delta_1,\Delta_2,\ldots,\Delta_M]^T$ and Δ_m is the time difference between two ears corresponding to the incidence angle ϕ_m of the input signal $p_m(t)$. The impulse response $h(t,\Delta_m)$ depends on the angle ϕ_m, due to the fact that for any signal $p_m(t)$ the equality $p_m(t-\Delta_m)*h(t)=p_m(t)*h(t-\Delta_m)$ always holds. Thus, it can be concluded that the system has different impulse responses and respective frequency responses for different incidence angles.

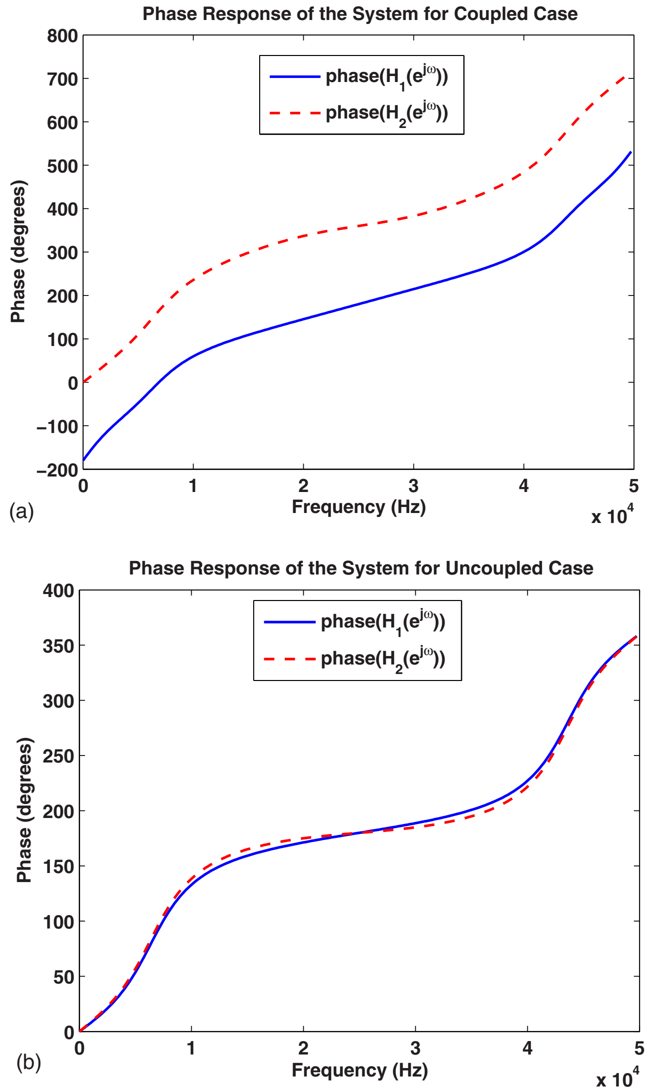

FIG. 4. (Color online) Phase responses of the *Ormia ochracea's* two ears. (a) Coupled system. (b) Uncoupled system.

It is assumed that $p_m(t)$ and $\boldsymbol{e}(t)=[e_1(t),e_2(t)]^T$ are zero-mean wide-sense stationary (WSS) Gaussian random processes; thus, $\boldsymbol{y}(t)$ is also a WSS Gaussian process since the system in Eq. (3) is linear and time invariant for zero initial state. These assumptions are used to asymptotically compute the CRB on the variance of the error of estimating the input signal incidence angle ϕ_m when there is an unbiased estimator $\hat{\phi}_m$ available.[14,15] However, for simplicity, the following further assumptions are made: $e_1(t)$ and $e_2(t)$ are white, have the same variance σ_e^2, and are uncorrelated with each other as well as with $p_m(t)$ $(m=1,2,\ldots,M)$. These assumptions result in

$$S_y(\omega,\boldsymbol{\Theta})=\sum_{m=1}^{M}\boldsymbol{H}(e^{j\omega},\Delta_m)S_{p_m}(\omega)\boldsymbol{H}^H(e^{j\omega},\Delta_m)+\sigma_e^2 I, \qquad (5)$$

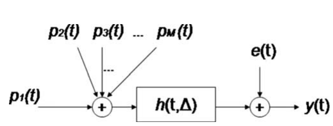

FIG. 5. Measurement model.

where

(i) $S_{p_m}(\omega)$, $\sigma_e^2 I$, and $S_y(\omega,\boldsymbol{\Theta})$ are the power spectral densities of $p_m(t)$, $\boldsymbol{e}(t)$, and $\boldsymbol{y}(t,\boldsymbol{\Delta})$, respectively;

(ii) $\boldsymbol{\Theta}=[\Delta_1,\Delta_2,\ldots,\Delta_M,S_{p_1},\ldots,S_{p_M},\sigma_e^2]^T$ $=[\Theta_1,\ldots,\Theta_{2M+1}]$; and

(iii) $\boldsymbol{H}(e^{j\omega},\Delta_m)=[H_1(e^{j\omega},\Delta_m),H_2(e^{j\omega},\Delta_m)]^T$ $(m=1,2,\ldots,M)$ is the frequency response vector of the system related to the input signal $p_m(t)$ with incidence angle ϕ_m and "$(.)^H$" denotes the Hermitian transpose.

B. Cramér–Rao bound

Let $\boldsymbol{y}(t,\boldsymbol{\Delta})$ be defined as in Eq. (4) and satisfy the assumptions defined in Sec. III A. Then, the elements of the Fisher information matrix corresponding to unknown parameter vector $\boldsymbol{\Theta}=[\Delta_1,\Delta_2,\ldots,\Delta_M,S_{p_1},\ldots,S_{p_M},\sigma_e^2]^T$ can be found (for large N) as follows:[14,15]

$$[J(\boldsymbol{\Theta})]_{kl}=\frac{N}{4\pi}\int_{-\pi}^{+\pi}\mathrm{tr}\left\{\frac{\partial S_y(\omega,\boldsymbol{\Theta})}{\partial\Theta_k}S_y^{-1}(\omega,\boldsymbol{\Theta})\frac{\partial S_y(\omega,\boldsymbol{\Theta})}{\partial\Theta_l}\times S_y^{-1}(\omega,\boldsymbol{\Theta})\right\}d\omega,$$

$$[J(\boldsymbol{\Theta})]_{kl}\approx\frac{1}{2}\sum_{n=1}^{N}\mathrm{tr}\left\{\frac{\partial S_y(n,\boldsymbol{\Theta})}{\partial\Theta_k}S_y^{-1}(n,\boldsymbol{\Theta})\frac{\partial S_y(n,\boldsymbol{\Theta})}{\partial\Theta_l}S_y^{-1}(n,\boldsymbol{\Theta})\right\}, \qquad (6)$$

where $S_y(n,\boldsymbol{\Theta})$ is the discrete Fourier transform (DFT) of the system output with frequency index n, which is obtained by sampling $S_y(\omega,\boldsymbol{\Theta})$ in the frequency domain.[13]

Recall that $\Delta_m=d\sin(\phi_m)/v$. Hence, to find the CRB of estimating the DOA, ϕ_m, the transformation formula[15] is utilized as follows:

$$\mathrm{Var}(\hat{\phi}_m)\geq\left[\left(\frac{\partial g(\boldsymbol{\Theta})}{\partial\boldsymbol{\Theta}}\right)J^{-1}(\boldsymbol{\Theta})\left(\frac{\partial g(\boldsymbol{\Theta})}{\partial\boldsymbol{\Theta}}\right)^T\right]_{mm}, \qquad (7)$$

where

(i) $\boldsymbol{g}(\boldsymbol{\Theta})=[g_1(\boldsymbol{\Theta}),\ldots,g_M(\boldsymbol{\Theta})^T]$, with the mth element defined as $g_m(\boldsymbol{\Theta})=\arcsin(v\Delta_m/d)$, and

(ii) $J(\boldsymbol{\Theta})$ is the Fisher information matrix with $[J(\boldsymbol{\Theta})]_{kl}$ as defined in Eq. (6) $(1\leqslant k,\ l\leqslant 2M+1)$.

IV. NUMERICAL RESULTS

The CRBs of estimating the DOAs for the coupled and uncoupled systems are compared to show the effect of the coupling. The following scenario for different signal to noise ratios (SNRs) is used.

It is assumed that in Eq. (4), $p_1(t)$ with incidence angle ϕ_1 is the incoming signal that is to be localized and similarly $p_m(t)$ and $\phi_m(t)$ $(m=2,3,\ldots,M)$ are the signal from the environment and corresponding incidence angle, respectively. For simulation purposes only, ϕ_m is randomly chosen (ϕ_m is uniform in $[-90°,90°]$). Accordingly, SNR is defined as

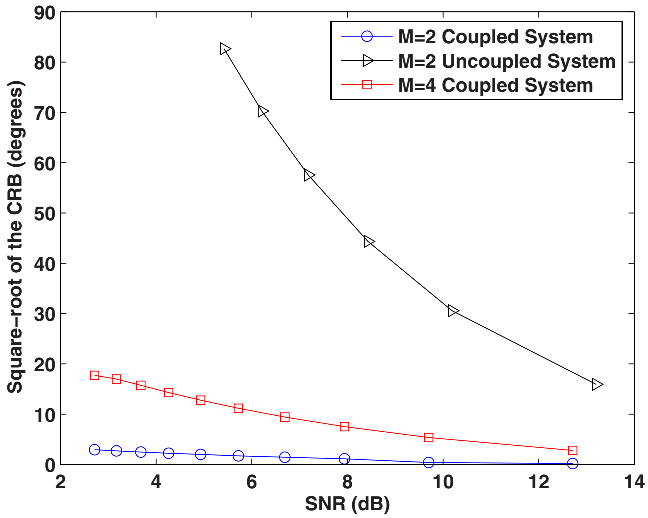

FIG. 6. (Color online) Square root of the CRB on the DOA estimation vs SNR.

$$\mathrm{SNR} = \frac{\mathrm{Tr}\{\Sigma_{n=1}^{N} \boldsymbol{H}(n,\Delta_1) S_{p_1}(n) \boldsymbol{H}^H(n,\Delta_1)\}}{\mathrm{Tr}\{\Sigma_{n=1}^{N}(\Sigma_{m=2}^{M} \boldsymbol{H}(n,\Delta_m) S_{p_m}(n) \boldsymbol{H}^H(n,\Delta_m)) + S_e(n)\}}, \tag{8}$$

that is, $p_m(t)$ for $m=2,3,\ldots,M$ contribute to the noise power. Note also that similar to Eq. (6) $\boldsymbol{H}(n,\Delta_m) = [H_1(n,\Delta_m), H_2(n,\Delta_m)]$ and $S_{p_m}(n)$ are the DFT of $\boldsymbol{H}(e^{j\omega},\Delta_m)$ and $S_{p_m}(\omega)$ and n denotes the frequency index.

In addition to the assumptions in Sec. III A, for further simplification, it is assumed that the spectrum corresponding to $p_m(t)$ is constant over the entire frequency range, i.e., $S_{p_m}(w) = \sigma_{p_m}$ $(\omega \in [-\pi, \pi])$. This simplification is reasonable in this problem since the amplitude response of the mechanical model is already selective (see Fig. 3).

- Model parameters[6] are chosen as follows:
  (1) $c_1 = c_2 = 1.15 \times 10^{-5}$ Ns/m and $k_1 = k_2 = 0.576$ N/m,
  (2) $c_3 = 3.88 \times 10^{-5}$ N s/m and $k_3 = 5.18$ N/m, and
  (3) $m = 2.88 \times 10^{-10}$ kg.
- Note also that in these examples
  (1) $\phi_1 = 45°$,
  (2) $t_0 = 0$ [See Eq. (3)], and
  (3) $T_s = 0.02$ ms is the sampling period.

In Fig. 6, the improvement on the lower bound of the error in estimating the DOA when there is coupling in the system is shown by plotting the square root of the CRB with respect to the SNR. This figure first illustrates the case where the number of the time samples is 2000 ($N=2000$), which correspond to a time range of 40 ms, and the number of input signals is 2 ($M=2$), i.e., there is only one interference signal other than the input itself. Note that the number of the time samples is chosen to obtain CRB values of roughly 1°–2° for the coupled system to match the experimental results in Ref. 10. When the CRBs of the coupled and the uncoupled system when $M=2$ are compared, a big difference is observed for the same SNR. This clear difference shows how the mechanical coupling improves the localization ability of the *O. ochracea*. For the coupled system the error in the azimuth angle drops down to 1°–2°, which is also in agreement with the experimental results demonstrated in Ref. 10. Note that for the uncoupled system when $M=2$, the variance of the error is markedly above the experimental results for SNR less than 12–14 dB.

Figure 6 also demonstrates the performance of only the coupled system with $N=5000$ and $M=4$. For the chosen values of M (the number of the input signals) and N (number of the time samples), the CRB values for the uncoupled system are too high, so the CRB does not hold anymore. $N=5000$ for $M=4$ are chosen in the same way described for $M=2$ to reach the desired CRB values. It is observed that as the number of interference signals increases, so does the number of time samples for the same CRB values, when the plots of the coupled system for $M=2$ and $M=4$ are compared. For the fly this may correspond to requiring more time to locate the source when background noise increases. It can also be seen from the same figure that to achieve the same CRB values as when $M=2$, higher SNR values are needed for when $M=4$.

V. CONCLUSION

The effect of coupling on the hearing system of the *O. ochracea* was analyzed. By examining the impulse and frequency responses of the model, it was shown that the coupling increased the time and amplitude differences between the two ears. Using our statistical model, the CRB of estimating the DOA for unknown input signal spectra was asymptotically computed. Comparing the CRB of the coupled with the uncoupled system, the enhancement provided by the mechanical coupling was illustrated. The experimental results regarding the azimuthal localization capacity of the *O. ochracea* were analytically proven. Future work will analyze the system and calculate the CRB in continuous time.

ACKNOWLEDGMENT

The authors are thankful to Dr. Chong Meng See of DSO, Singapore, for introducing them to the subject of the *Ormia ochracea's* hearing system. This work was supported by the DARPA Grant No. HR0011-07-1-0036.

[1] N. H. Fletcher and S. Thwaites, "Acoustical analysis of the auditory system of the cricket *Teleogryllus commodus* (walker)," J. Acoust. Soc. Am. **66**, 350–357 (1979).
[2] A. Michelsen, A. V. Popov, and B. Lewis, "Physics of directional hearing in the cricket *Gryllus bimaculatus*," J. Comp. Physiol., A **175**, 153–164 (1994).
[3] D. Robert, R. N. Miles, and R. R. Hoy, "Tympanal mechanics in the parasitoid fly *Ormia ochracea*: Intertympanal coupling during mechanical vibration," J. Comp. Physiol., A **183**, 443–452 (1998).
[4] A. R. Palmer and A. Pinder, "The directionality of the frog ear described by a mechanical model," J. Theor. Biol. **110**, 205–215 (1984).
[5] A. Michelsen, "Hearing and sound communication in small animals: Evolutionary adaptations to the laws of physics," *The Evolutionary Biology of Hearing* (Springer-Verlag, New York, 1992).
[6] R. N. Miles, D. Robert, and R. R. Hoy, "Mechanically coupled ears for directional hearing in the parasitoid fly *Ormia ochracea*," J. Acoust. Soc. Am. **98**, 3059–3070 (1995).
[7] D. Robert, R. N. Miles, and R. R. Hoy, "Directional hearing by mechanical coupling in the parasitoid fly *Ormia ochracea*," J. Comp. Physiol., A

179, 29–44 (1996).
[8]D. Robert, M. P. Read, and R. R. Hoy, "The tympanal hearing organ of the parasitoid fly *Ormia ochracea* (diptera, tachinidae, ormiini)," Cell Tissue Res. **275**, 63–78 (1994).
[9]D. Robert, M. J. Amoroso, and R. R. Hoy, "The evolutionary convergence of hearing in a parasitoid fly and its cricket host," Science **258**, 1135–1137 (1992).
[10]A. C. Mason, M. L. Oshinsky, and R. R. Hoy, "Hyperacute directional hearing in a microscale auditory system," Nature (London) **410**, 686–690 (2001).
[11]K. Ogata, *Modern Control Engineering*, 4th ed. (Prentice-Hall PTR, Upper Saddle River, NJ, 2001).
[12]W. E. Boyce and R. C. Diprima, *Elementary Differential Equations and Boundary Value Problems*, 7th ed. (Wiley, New York, 2000).
[13]A. V. Oppenheim, R. W. Schafer, and J. R. Buck, *Discrete-Time Signal Processing*, 2nd ed. (Prentice-Hall PTR, Upper Saddle River, NJ, 1999).
[14]P. Whittle, "The analysis of multiple stationary time series," J. R. Stat. Soc. Ser. B (Methodol.) **15**, 125–139 (1953).
[15]S. M. Kay, *Fundamentals of Statistical Signal Processing: Estimation Theory* (Prentice-Hall PTR, Upper Saddle River, NJ, 1993).